Development and Characterization of Thermosensitive Hydrogels Based on Poly(*N*-isopropylacrylamide) and Calcium Alginate

Stojanka Petrusic,[1,2,3] Maryline Lewandowski,[1,2] Stéphane Giraud,[1,2] Petar Jovancic,[3] Branko Bugarski,[3] Sanja Ostojic,[4] Vladan Koncar[1,2]

[1]*Univ Lille Nord de France, F-59000 Lille, France*
[2]*Ecole Nationale Supérieure des Arts et Industries Textiles, GEMTEX, F-59100 Roubaix, France*
[3]*Faculty of Technology and Metallurgy, University of Belgrade, Belgrade, Serbia*
[4]*Institute of General and Physical Chemistry, Belgrade, Serbia*

Received 20 July 2010; accepted 20 June 2011
DOI 10.1002/app.35122
Published online 10 October 2011 in Wiley Online Library (wileyonlinelibrary.com).

ABSTRACT: This work refers to the synthesis and characterization of thermosensitive hydrogels based on interpenetrating polymer networks (IPNs) of poly(*N*-isopropylacrylamide) (PNIPAAm) and calcium alginate in the form of films. The influence of the crosslinking degree of PNIPAAm and alginate content on thermal, swelling, mechanical, and morphological properties of hydrogels is investigated in detail. Characterization of pure PNIPAAm hydrogels and IPN hydrogels was performed by FTIR, DSC, DMA, and SEM. In addition, the studies of equilibrium swelling behavior as well as swelling, deswelling, and reswelling kinetics are performed. The results obtained imply the benefits of synthesizing IPNs based on PNIPAAm and calcium alginate over pure PNIPAAm hydrogels. The presence of calcium alginate contributes to the improvement of mechanical properties, the deswelling rate of hydrogels, and the network porosity, without altering the thermosensitivity of PNIPAAm significantly.
 J Appl Polym Sci 124: 890–903, 2012

Key words: thermosensitive hydrogels; interpenetrating polymer network (IPN); swelling behavior; mechanical properties; morphology

INTRODUCTION

Hydrogels represent three-dimensional polymeric networks capable of swelling in water or other biological fluid while retaining great amounts of liquid. These polymeric materials may absorb from 10% to 20% up to thousands of times their dry weight in water.[1] What distinguish hydrogels from other polymeric materials are unique properties like soft and rubbery consistency, low interfacial tension with water or other biological fluids, and considerable percentage of water in structure. These characteristics make hydrogels an important class of biocompatible polymers.

At present, the greatest attention in research is put on the class of hydrogels exhibiting considerable changes in their swelling behavior, network structure, permeability, or mechanical strength in response to very slight changes in their environment.[2] The stimulus can be for instance pH, temperature, electric field, or ionic strength. Among these environmentally-responsive hydrogels, thermosensitive hydrogels have found the broadest application, primarily because of the fact that temperature is an operational parameter that can be easily controlled. In addition, this type of hydrogels does not require any chemical stimulus, besides temperature to respond.

Among various biomedical applications of hydrogels,[1] drug release systems represent a particularly attractive field, with regard to the possibility of controlling and modifying drug release profile.[3] Hydrogels of thermoshrinking type[4] are characterized by a lower critical solution temperature (LCST) above which they contract, which makes them suitable for the drug release systems and arouses our interest in their application. The most exploited hydrogel in this group is crosslinked poly(*N*-isopropylacrylamide) (PNIPAAm), widely used in many fields because of its convenient LCST, between 30°C and 35°C.[5] PNIPAAm exhibits volume phase transition as a result of the breakdown of delicate hydrophilic/hydrophobic balance within polymer network because of the presence of both hydrophilic amide groups and hydrophobic isopropyl groups in its side chains.[6] At lower temperatures, hydrogen bonding between hydrophilic segments of the polymer chain

Correspondence to: S. Petrusic (spetrusic@tmf.bg.ac.rs).
Contract grant sponsor: Ministry of Science of Republic of Serbia; contract grant number: III46010.
Contract grant sponsor: French Ministry of Foreign Affairs and the Region Nord-Pas-De-Calais.

and water molecules dominates. At elevated temperatures, hydrophobic interactions among hydrophobic segments become stronger whereas hydrogen bonds weaken and break. This leads to deswelling (shrinking) of hydrogels due to interpolymer chain association through hydrophobic interactions.[7]

Our general aim is to develop thermosensitive hydrogels as transdermal drug delivery matrices combined with a heating textile, already described by Koncar et al.[8] Therefore, in this work, as a first step of the broader research, we focused on synthesis and detailed characterization of hydrogels composed of PNIPAAm and calcium alginate (CA). CA is a physical hydrogel that is not thermosensitive, but it has been widely used in drug release studies with regard to its biocompatibility and particularly mild conditions of preparation.[9,10] CA is typically prepared by crosslinking of sodium alginate with Ca^{2+} ions. Commercially available sodium salt of alginate is biodegradable linear copolymer of (1-4)-linked α-L-guluronic acid (G) and β-D-mannuronic acid (M) that shows characteristic ion binding affinity toward multivalent cations, resulting in gelling and formation of a network.[11]

It is well known that limitations in application of pure PNIPAAm hydrogels mainly come from their poor mechanical properties. This could be overcome by PNIPAAm copolymerization with other components or by formation of full- and semi-interpenetrating polymer networks.[12–14] The formation of full-interpenetrating polymer networks (IPNs) represents the only way to combine crosslinked polymers. It results in relatively dense hydrogel matrices featuring stiffer and tougher networks with more widely controllable physical properties.[3] There are a number of reports referring to linear alginate (sodium alginate) in combination with crosslinked PNIPAAm having structures of semi-IPNs,[15–18] as well as to IPN hydrogels containing crosslinked PNIPAAm and CA.[19–23] The reports on PNIPAAm/CA hydrogels do not show that in addition to mechanical properties, IPN hydrogels could also feature improved swelling behavior and better response to temperature changes than pure PNIPAAm hydrogel. The major part of the published studies characterizes the IPN hydrogels with respect to pure CA hydrogels. Therefore, in our research, we underlined the advantages of PNIPAAm/CA over the pure PNIPAAm hydrogels. By this approach, it is possible to synthesize specific PNIPAAm/CA hydrogels with improved mechanical properties, more porous structure, and faster deswelling rate without affecting the LCST. This could be of great importance for the development of thermosensitive hydrogels as transdermal drug delivery matrices in the next research step.

EXPERIMENTAL

Materials

N-isopropylacrylamide (NIPAAm, 97%, from ς-Aldrich) was purified by recrystallization in *n*-hexane before use. *N,N,N′,N′*-tetramethylethylenediamine (TEMED, 99%), *N,N′*-methylenebis(acrylamide) (MBAAm, 99%), sodium alginate salt (low viscosity) were also supplied by Sigma-Aldrich, ammonium persulphate (APS) by Prolabo, and calcium chloride ($CaCl_2$, 95%) by Panreac.

Preparation of hydrogel films

Two types of hydrogel films were prepared: pure poly(*N*-isopropylacrylamide) (PNIPAAm) as well as IPNs based on PNIPAAm and calcium alginate (CA). The synthesis implied the polymerization of NIPAAm by free-radical polymerization mechanism and chemical crosslinking with MBAAm. In the case of IPN films, (sodium) alginate was crosslinked in the presence of two-valent calcium ions by means of ionic interactions. In the following, all quantities in wt % are based on the amount of monomer (NIPAAm) used.

Initially, an aqueous solution of 5 wt % NIPAAm monomer and crosslinker MBAAm (2 and 3 wt %) was prepared and purged with nitrogen for 30 min and kept on a magnetic stirrer in an ice-water bath. Afterwards, an initiator, APS (1 wt %), and a catalyst, TEMED (1 wt %), were added. The synthesis of IPNs based on PNIPAAm and CA was performed according to the same principle, with a difference in the first step, which implied dissolution of predetermined amount of sodium alginate in distilled water prior to adding NIPAAm and MBAAm.

In both cases, the final reaction solution (shortly after addition of APS and TEMED) was injected with a syringe in a glass mold composed of two glass plates separated by a 1.5 mm thick gasket. The molds were left for 24 h in refrigerator. Afterwards, in the case of pure PNIPAAm, the films were removed from the molds and placed in distilled water. Concerning the IPN-hydrogel films, instead of water, the molds were placed into 1.5 *w/v* % aqueous solution of $CaCl_2$, after removing gaskets, for 24 h. Then the films were removed from the glass plates and were placed into a fresh $CaCl_2$ solution for another 24 h.

Finally, all synthesized hydrogel films were kept in fresh distilled water with daily refreshment for a week, with the purpose of purification and removal of excess reagents. Eight different hydrogel films were prepared: two pure PNIPAAm films (P-0-5-2 and P-0-5-3) and six IPN films based on PNIPAAm and CA (IPN-1-5-2, IPN-2-5-2, IPN-3-5-2, IPN-1-5-3, IPN-2-5-3 and IPN-3-5-3). Letters P and IPN in the name codes describe pure PNIPAAm network and

interpenetrating polymer network, respectively. The first number stands for the weight fraction of sodium alginate, the middle one defines the weight fraction of the monomer NIPAAm, and the last one represents the weight fraction of the crosslinker MBAAm based on the weight of NIPAAm, all referring to the composition of the initial reaction solutions.

Characterization methods

FTIR and elemental analysis

FTIR spectroscopy was used to analyze the chemical structure of hydrogel films, and thus examine the presence of both PNIPAAm and CA in the final 3D network. Hydrogel film samples were first dried in a vacuum oven at 60°C until reaching constant weight. They were then ground into fine powder, mixed, further ground with potassium bromide and pressed into pellets. FTIR spectra were recorded in transmission mode using a BOMEM spectrometer (Hartmann and Braun) in the range 4000–600 cm^{-1} and with a resolution of 4 cm^{-1}. Elemental analysis of selected xerogels was performed on a VARIO EL III elemental analyzer (Elementar).

DSC thermal analysis

A differential scanning calorimeter (2920 Modulated DSC, TA Instruments) was used to determine the lower critical solution temperature (LCST), as well as glass transition temperature (T_g) of the hydrogels. In both analyses, the scans were performed in duplicates.

For determination of the first parameter, LCST, a temperature ramp was performed on the sample, from 20°C to 50°C, at a heating rate of 3°C min^{-1}, and under a nitrogen flow of 50 mL min^{-1}. All runs were conducted in hermetically sealed aluminum pans, with distilled water used as a reference material. Calibration was performed using high purity indium as standard. Temperature of the endothermic maximum was referred to as the LCST or volume phase transition temperature.[24]

For determination of the glass transition temperature (T_g) the samples were dried under vacuum until reaching a constant weight. Each sample was placed in hermetically sealed aluminum pan, while the reference pan was empty. The scanning procedure involved initial heating from 20°C to 200°C at a rate of 20°C min^{-1} for the removal of any thermal history and residual moisture. Immediately afterwards the samples were exposed to cooling down to 10°C at a rate of 10°C min^{-1}, and this was followed by reheating from 10°C to 200°C at a rate of 20°C min^{-1}. The scans were conducted under a nitrogen flow of 50 mL min^{-1} and calibration was performed using high purity indium as standard. The T_g was determined as the inflection point of the endothermic drift in the second heating curve of thermogram.

Swelling behavior

Swelling behavior of hydrogels was studied through the dependence of the equilibrium swelling ratios on temperature, kinetics of swelling from the dried state, kinetics of deswelling, and kinetics of reswelling. The hydrogel samples were punched from the films in the form of disks and further used in the gravimetrical measurements of the swelling characteristics in distilled water.

Equilibrium swelling ratio (ESR) of hydrogels over a range of temperatures (from 25°C to 50°C) was obtained after the incubation of hydrogels in thermostated water until they reached equilibrium swollen state. ESR was calculated according to the following formula:

$$\mathrm{ESR}\,(\%) = \frac{W_s - W_d}{W_d} \times 100 \qquad (1)$$

where W_s represents the weight of equilibrium swollen hydrogel disk at a given temperature and W_d the weight of the dried gel (xerogel). The weight of the swollen hydrogel was measured after blotting the excess surface water with wet filter paper. The weight of the xerogels was obtained after drying the samples under vacuum at 60°C until reaching constant weight.

Swelling kinetics was investigated when completely dried samples were immersed in thermostated water at 25°C and their weight was measured at predetermined time intervals. For the study of deswelling kinetics, the hydrogels were allowed to swell to equilibrium in water at 25°C, and then they were transferred into thermostated water at 40°C, and periodically weighed. Reswelling kinetics of hydrogels was obtained by immersing preweighed equilibrium swollen hydrogels at 40°C in thermostated water at 25°C and weighing them at predetermined time intervals. Swelling and reswelling kinetics of hydrogels were interpreted through the percentage of water uptaken (WU) over the dry weight of hydrogel, using the following equation:

$$\mathrm{WU}\,(\%) = \frac{W_t - W_d}{W_d} \times 100 \qquad (2)$$

where W_t is the weight of hydrogel at predetermined time interval. Deswelling kinetics was presented using percentage of water retained (WR) over the dry weight of hydrogel using the equivalent equation. The values of ESR, WU, and WR were calculated as the average of three measurements.

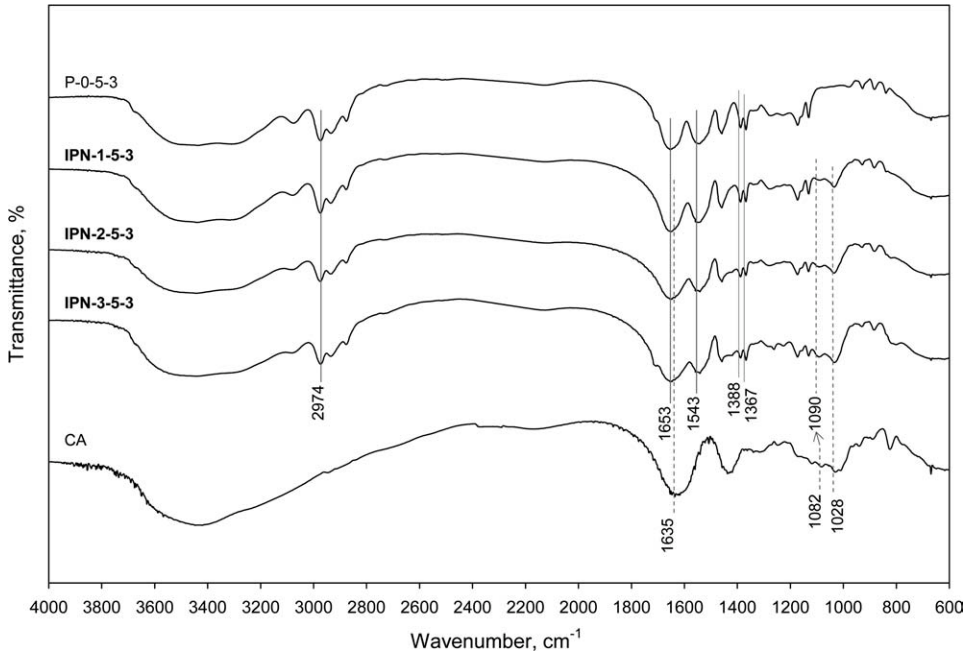

Figure 1 FTIR spectra (characteristic peaks of PNIPAAm chains indicated by full lines and those of CA network by dotted lines).

Mechanical characterization

Mechanical testing was performed in compression mode on a Dynamic Mechanical Analyzer (Q800, TA Instruments). The storage and loss moduli of hydrogel disk samples below and above their LCST (at 30°C and 40°C, respectively) were examined. Frequency sweeps from 1–100 Hz were performed on swollen hydrogel disk samples under preload force of 0.5 N and at a strain amplitude of 10 μm. The hydrogel disks were around 13 mm in diameter and they were blotted with wet filter paper before each analysis. In addition, circular pieces of a thin nonwoven fabric were placed on top and bottom surfaces of the circular clamps of the assembly for compression testing to avoid the lubricant effect of water layer between the hydrogel surface and steel clamp surfaces.

Morphology analysis

The morphology of the freeze-dried hydrogels disks was analyzed using a Scanning Electron Microscope (JEOL 5800 SEM, JEOL). The aim was to obtain information about the pore structure of hydrogels in the swollen state below and above their LCST. Hence, the samples were incubated in distilled water at 25°C and at 40°C for 48 h before a treatment in a freeze-dryer (GAMMA 1-16 LSC, Martin Christ) for 48 h. Freeze-drying process included freezing at −30°C followed by primary vacuum drying at −23°C and secondary vacuum drying at 20°C. Prior to SEM observation, cross section of the freeze-dried hydrogel disks was coated with Ag-Pt-Pd alloy by sputtering for 30 s. The average pore sizes of hydrogels were determined using a software, SmartTiff Image Viewer V1.0.0.10 (Carl Zeiss SMT, Ltd), based on 70 analyzed pores per image.

RESULTS AND DISCUSSION

FTIR and elemental analysis

The results of FTIR analysis are presented in Figure 1. The samples of pure CA, based on 3 wt % sodium alginate were also examined for comparison.

In the spectra of P-0-5-3, IPN-1-5-3, IPN-2-5-3, IPN-3-5-3, characteristic absorptions of PNIPAAm are observed, the amide I band at 1653 cm^{-1} (C═O stretching) and amide II band at 1543 cm^{-1} (N─H bending) of the amide group.[25] The bands at 1388 and 1367 cm^{-1} are assigned to C─H vibrations of isopropyl group of PNIPAAm.[12] Another characteristic absorption band of PNIPAAm, clearly seen in the spectra of all IPN samples, appears around 2974 cm^{-1} and is attributed to the C─H stretching vibration of ─CH─ bridges of PNIPAAm network.[25] Thus, the successful polymerization of NIPAAm was verified. This is supported by the fact that characteristic peaks of this monomer are not present in the corresponding spectra, primarily implying the bands at 1617 cm^{-1} (C═C), at 1409 cm^{-1} (CH_2═), as reported elsewhere.[26]

The characteristic asymmetric stretching vibration of COO^- groups in CA network is manifested through the peak 1635 cm^{-1}.[27,28] In the spectra of

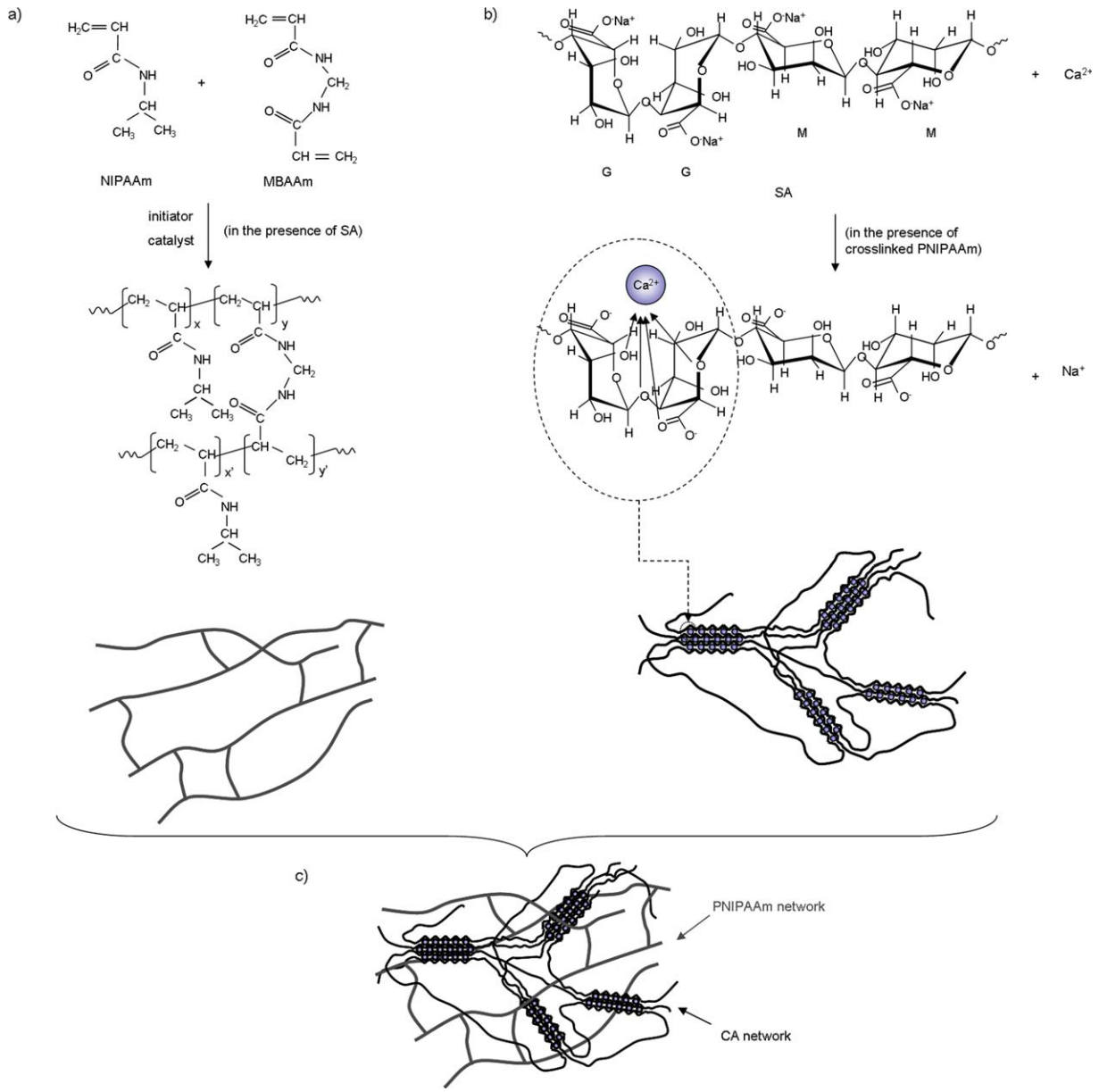

Figure 2 Formation of the IPN hydrogel structure: copolymerization/crosslinking of NIPAAm (Adapted from Ref 31, with permission from Wiley) (a), crosslinking of alginate (b), and resulting PNIPAAm/CA IPN structure (c). [Color figure can be viewed in the online issue, which is available at www.wileyonlinelibrary.com.]

IPNs, this peak is hidden by a broad amide II band of PNIPAAm at 1653 cm^{-1}, as noted earlier. The absorbance at 1082 and 1090 cm^{-1} in the spectra of CA and IPNs, respectively, is a result of C—O—C stretching of the pyranose ring in mannuronate (M) and guluronate (G) residues.[29] The band at around 1028 cm^{-1} in spectra of CA and IPNs is assigned to O—H bending vibrations,[29] as well as to C—O stretching of alginate structural units.

In all analyzed spectra, a broad peak between 3600 and 3200 cm^{-1} is present because of O—H stretching vibrations, primarily as a sign of moisture absorption. Concerning CA and IPNs, this broad peak arouses from hydroxyl groups in G and M residues of alginate chain, indicating the formation of intermolecular hydrogen bonding.[30] Furthermore, in the case of P-0-5-3 and IPNs, there is contribution of N—H stretching of the repeating units of NIPAAm in the same range.[25] Hence, FTIR analysis confirmed the presence of both polymer networks, crosslinked PNIPAAm and CA, in IPN samples. Figure 2 is representing the probable reaction scheme for the formation of crosslinked PNIPAAm in the presence of sodium alginate (SA), the subsequent step of the crosslinking of alginate by calcium ions according to the egg-box model,[32] and finally resulting IPN structure.

Results of elemental analysis of nitrogen performed on selected samples are given in Table I. As

TABLE I
Elemental Analysis Results

Hydrogel	N_{the} (wt %)	N_{exp} (wt %)	$(N_{the} - N_{exp})/N_{the} \times 100$ (%)
P-0-5-2	12.49	12.15	2.72
IPN-1-5-2	10.47	10.12	3.34
IPN-2-5-2	9.01	8.57	4.92

expected, nitrogen content decreases with decrease in NIPAAm fraction. By comparing theoretical and experimental % N it can be concluded that less NIPAAm is incorporated in the polymer network with an increase in alginate fraction.

Lower critical solution temperature

The results obtained by DSC (Fig. 3) show that all hydrogel films exhibit the LCST values around 34°C–35°C, i.e., the volume phase transition temperature is not considerably influenced by the presence of CA chains or by the degree of PNIPAAm crosslinking.

In comparison with pure PNIPAAm hydrogel with lower crosslinking degree, formation of the IPN structures based on 1 and 2 wt % alginate has not resulted in change of the LCST, whereas IPN-3-5-2 exhibited slightly higher LCST [Fig. 3(a)]. Incorporation of CA network was expected to give prominent rise to the LCST values of the final structures because of greater number of hydrophilic groups of alginate chains. However, close LCST values of homopolymer hydrogels (P-0-5-2 and P-0-5-3) and IPN hydrogels mean that the presence of alginate chains in IPN hydrogels does not provide enough interactions to influence the hydrophilic/hydrophobic balance of PNIPAAm chains. This could be explained by the formation of a complex between the carboxylic groups of alginate and the amide groups of PNIPAAm, which is responsible for the reduced hydrophilicity of the IPNs than expected in comparison with alginate fraction.[33] Furthermore, the number of hydroxyl groups in alginate chains that rises with increase in alginate fraction could not induce proportional increase in number of hydrogen bonds between them and water molecule because of tighter network structure that could not accommodate great amounts of water. Additional reason for negligible differences in the LCST of analyzed hydrogels might lie in relatively high monomer concentration for the preparation of hydrogels. Similar study of PNIPAAm hydrogel networks interpenetrated with CA networks showed that only at low initial NIPAAm monomer concentration (2.5 wt %), the phase transition is favored at higher temperatures because of easier motion of PNIPAAm chains.[20] This requires greater energy for driving hydrophilic–hydrophobic transition, and hence it should result in higher LCST. Also, DSC analysis indicated that the structure of each network forming the IPN is retained during the synthesis since the incorporation of CA does not cause any significant deviation from the LCST of pure PNIPAAm network.[34]

The obtained results also show that the PNIPAAm crosslinker (MBAAm) content does not significantly influence the LCST of the hydrogel, since increasing its concentration from 2 to 3 wt % in the feed solution (i.e., molar ratio of NIPAAm and MBAAm is decreased from 68.1 to 45.4) causes negligible rise in the LCST values of corresponding IPN samples. The highest difference in the LCST values (0.9°C) is obtained for analogous samples based on 1 and 2 wt % of alginate.

Glass transition temperature

Literature values of the glass transition temperature of linear PNIPAAm range between 85 and 130°C.[35] With regard to crosslinked PNIPAAm, the results obtained by Zhang et al.[14] indicate a T_g of 131.4°C for the PNIPAAm hydrogel based on 6.7 wt % monomer solution with 2 wt % crosslinker MBAAm (based on monomer), which is close to our results for both P-0-5-2 and P-0-5-3 (Fig. 4).

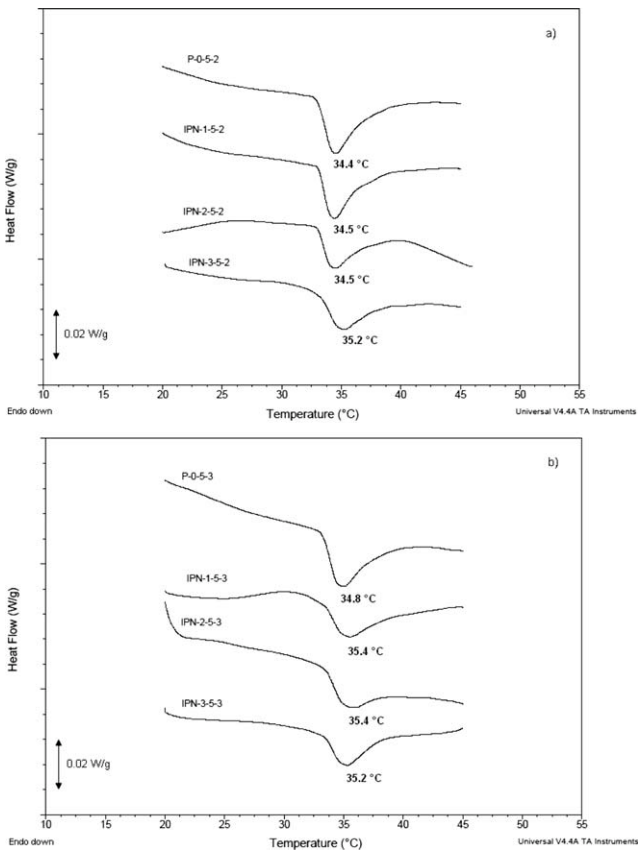

Figure 3 DSC thermograms for determination of the LCST of hydrogels with lower (a) and higher (b) crosslinking degree of PNIPAAm.

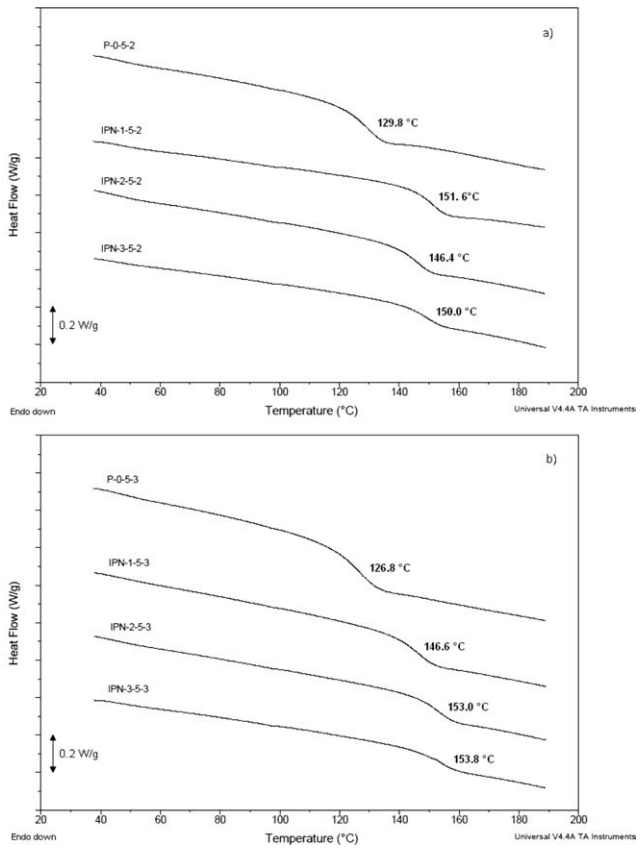

Figure 4 DSC thermograms for determination of T_g values of hydrogels with lower (a) and higher (b) crosslinking degree of PNIPAAm.

In the case of PNIPAAm crosslinked by gamma radiation, noticeably higher values of the T_g were reported,[36] e.g., a T_g of 149°C was obtained for a PNIPAAm hydrogel based on 10 wt % monomer solution and irradiated at 70 kGy with a 60-Co source, signifying stronger network in comparison with a chemically crosslinked PNIPAAm. Our study shows that the CA network considerably contributes to the improved stability of the final IPNs, in contrast to pure chemically crosslinked PNIPAAm hydrogel. An increase in fraction of the second network (CA) results in the increase in T_g values, owing to hindering of the chain mobility, with the exception of the sample IPN-1-5-2, whose T_g value is unexpectedly higher.

The IPNs are characterized by strong interactions among polymer chains, since a temperature above 153°C in the case of IPN-2-5-3 and IPN-3-5-3 is necessary to promote the chain mobility [Fig. 4(b)]. This T_g value can be compared to the T_g of 149.7°C obtained for hydrogels composed of two interpenetrating networks of PNIPAAm.[14] Therefore, CA network leads to the improvement in strength of the interactions on a molecular level when it is combined with PNIPAAm to form IPN.

Swelling behavior

Equilibrium swelling ratio of hydrogels

Thermosensitivity of synthesized hydrogels was expressed through the values of equilibrium swelling ratio (ESR) over the range of temperatures from 25°C up to 50°C. The swelling profiles in Figure 5 indicate that the ESR of the IPN samples at lower temperatures (<31°C) is decreasing with increase in alginate concentration because of reduced mobility of PNIPAAm chains in these more compact hydrogel networks. Furthermore, there is a noticeable difference in the ESR at 25°C between the samples with different crosslinking degree of PNIPAAm. Higher concentration of crosslinks in PNIPAAm network of IPN-1-5-3 resulted in around 18% lower ESR, in comparison with IPN-1-5-2. The ESR value of pure PNIPAAm hydrogels (2250% and 1983% for P-0-5-2 and P-0-5-3, respectively) is lower than those of IPN hydrogels based on 1 wt % alginate (2450% and 2134% for IPN-1-5-2 and IPN-1-5-3, respectively), which indicates the ability of the latter hydrogels to

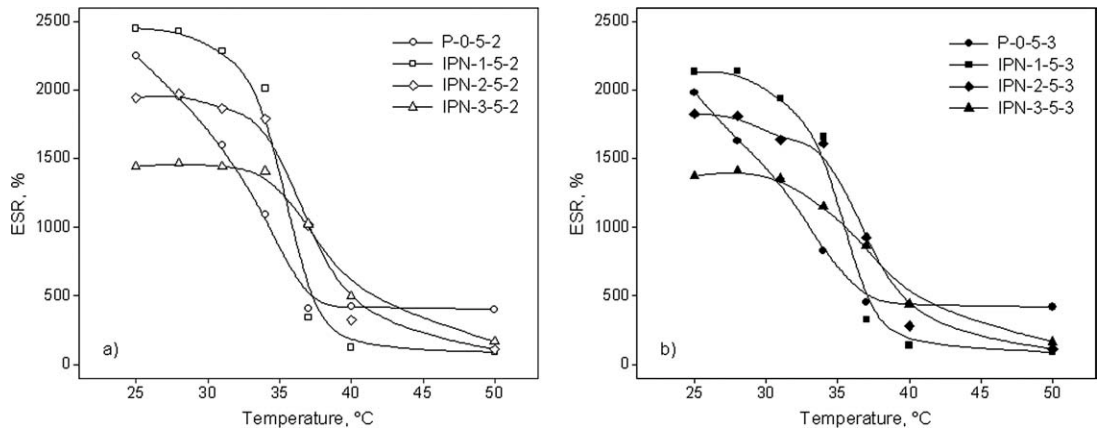

Figure 5 Equilibrium swelling ratio of hydrogels with lower (a) and higher (b) crosslinking degree of PNIPAAm as a function of temperature.

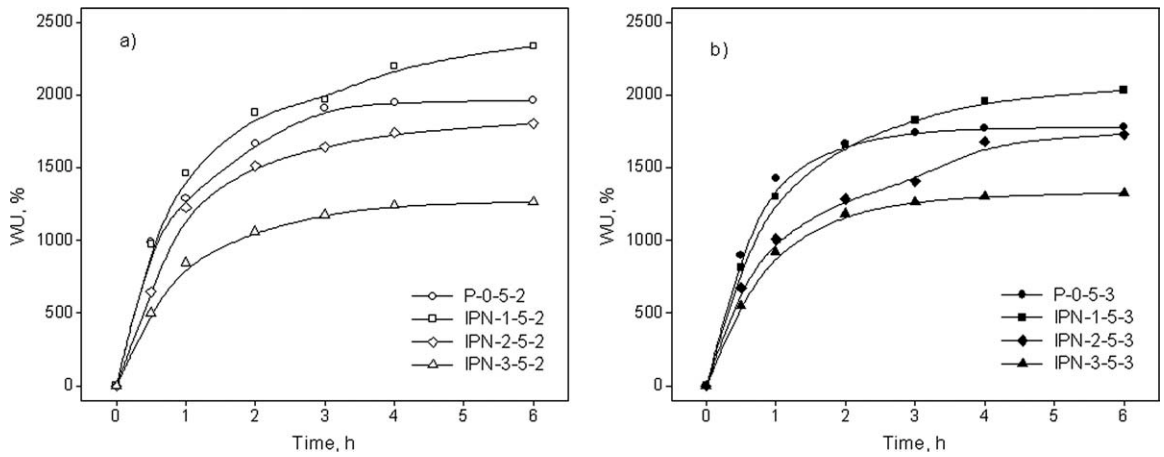

Figure 6 Swelling kinetics of dried hydrogels with lower (a) and higher (b) crosslinking degree of PNIPAAm at 25°C.

accommodate more water. This was confirmed by SEM analysis and calculation of the average pore size of the samples at 25°C (Fig. 13). More developed porous structure of IPN-1-5-*x* than P-0-5-*x* ($x = 2, 3$) provided higher water swelling capacity. The analogous conclusion could be deduced for the relation of the ESR and the average pore size at 40°C.

The difference in ESR at lower temperatures (25°C, 28°C) between two hydrogels with higher fraction of alginate (IPN-3-5-2 and IPN-3-5-3) is only slightly pronounced because of predominant influence of CA network. It probably masks the differences arousing from different crosslinking degree of the other network (PNIPAAm) in IPNs. The concentration of crosslinker MBAAm in hydrogels with the same amount of alginate affects neither the general shape of the curve, nor the LCST values that could be determined from the inflection point of each swelling curve. It is estimated that the LCST increases depending on the presence and moiety of CA in IPN hydrogels. The LCST of IPN hydrogels based on 2 and 3 wt % of alginate are close to 37°C, which is not in well agreement with the DSC results, since the different methods of measurement can give changes in this temperature of even 4°C.[37]

Obtained swelling profiles confirms known property of pure PNIPAAm hydrogels to have weaker response to temperature variations, as a result of the formation of a skin layer.[38,39] This dense skin layer hinders the diffusion of water molecules out of the gel during the deswelling process at higher temperatures (>LCST). Addition of alginate as a hydrophilic component, primarily because of hydroxyl groups, reduces hydrophobic aggregation in the surface layer of hydrogel and formation of the skin layer. It reflects in higher rate of decrease of the ESR with increase temperature of IPN hydrogels. The sharpest volume phase transition exhibits hydrogel IPN-1-5-2, whose ESR rapidly decreases once the LCST (34.5°C) is exceeded and drops from 2011% down to 123% between 34°C and 40°C, respectively, [Fig. 5(a)]. Hydrogels with higher fraction of alginate have slower response rate than IPN-1-5-2 and IPN-1-5-3. This could be explained by stronger interactions (hydrogen bonds) between hydrogen of hydroxyl groups of alginate and nitrogen of amide groups of PNIPAAm, due to more compact and denser IPN structures, and hence, weaker influence on the reduction of hydrophobic aggregation in surface layer.

An increase in alginate content in IPN hydrogels leads to the reduced mobility of PNIPAAm chains in these networks and consequently weaker water uptake ability, as was also the case in similar systems.[19] It is shown that different concentration of alginate in the feed mixture influences swelling properties of IPN hydrogels. Degree of PNIPAAm crosslinking impacts the ESR at lower temperatures. This is confirmed by SEM analysis, and presented through the values of the average pore size at 25°C and 40°C (Fig. 13). After exhibiting phase transition, well above the LCST (at 50°C), the IPN hydrogels show relatively similar ESR values, which indicates the transition of their network into a similar tightly compact structure.

Swelling kinetics

When dried PNIPAAm and IPN gels are immersed in water at 25°C, they all show similar swelling trend (Fig. 6). The rates of swelling are high during the first hour and than gradually decrease until the equilibrium swelling is reached. The difference between the osmotic pressure in the bulk water and in the swelling samples is the highest at the beginning of the process and it decreases with time. The first hour of swelling was characterized by high water uptake rate that is governed by the diffusion of water molecules into the dry sample. This is followed by the relaxation of the hydrated polymer chains and finally expansion of the hydrogel network.[40] Therefore, all given profiles are marked by

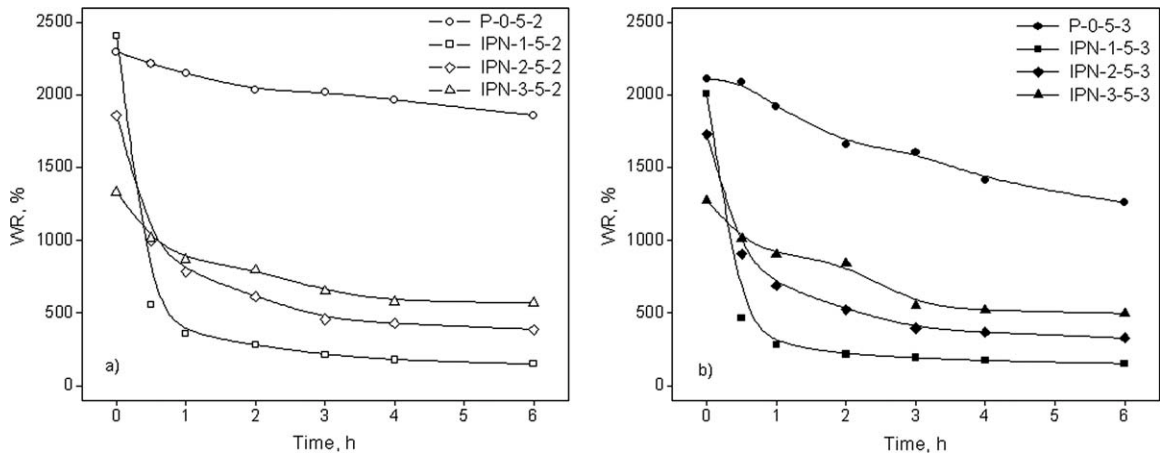

Figure 7 Deswelling kinetics of hydrogels with lower (a) and higher (b) crosslinking degree of PNIPAAm at 40°C.

slow second phase of swelling. After the initial 30 min of swelling, the highest increase in water uptake in comparison with the equilibrium state showed pure PNIPAAm hydrogels (45%) and after them IPN-1-5-2 (41%), reaching WU close to 1000%. These samples have the least compact dried structure with the lowest polymer chain per unit volume, which enables easier water penetration into the gel. Increased presence of alginate network affected slower swelling process so that WU of IPN-2-5-2 and IPN-3-5-2 equaled 1515% and 1061% (respectively), in comparison with 1666% of P-0-5-2 after the second hour of swelling. Measurements of the swelling kinetics up to 48 h indicated that the equilibrium swelling time is slightly shortened when the fraction of alginate in IPNs is raised. The impact of crosslinking degree of PNIPAAm is negligible for the IPN samples with high alginate concentration and it is the most pronounced for IPN based on 1 wt % alginate.

Deswelling kinetics

The kinetics of water loss from hydrogels at elevated temperature, displayed in Figure 7, clearly indicates rather slow shrinking rate of pure PNIPAAm hydrogels in comparison with other samples. In general, formation of IPN structures considerably enhanced the deswelling rate of the hydrogels. The percentage of water retained of P-0-5-2 and P-0-5-3 decreased around 9% and 19% (respectively) after 2 h of deswelling at 40°C compared with the initial state at 25°C. As opposed to them, IPN hydrogels based on 1 and 2 wt % alginate showed considerably higher deswelling ability within the same period. Decrease in WR was more than 80% in 2 h for IPN-1-5-2 and IPN-1-5-3. As already noted, the incorporation of CA network weakens the hydrophobic interactions among isopropyl groups of PNIPAAm in the surface layer. Thus, the formation of dense skin layer (which blocks the outflux of entrapped water from the hydrogel network) is weakened, leading to a higher deswelling rate of IPNs. Rapidly structured skin phase of P-0-5-2 and P-0-5-3 does not allow the water molecules inside these hydrogels to be easily squeezed out. Hence, the equilibrium state is achieved slowly. Pure PNIPAAm hydrogels reach equilibrium at 40°C after 48 h, whereas IPN hydrogels needs around 4 h. The given deswelling profiles near equilibrium state correspond to the pore structure of hydrogels at 40°C, i.e., their average pore size that decrease in the order P-0-5-x > IPN-3-5-x > IPN-2-5-x > IPN-1-5-x (Fig. 13).

When comparing deswelling behavior of IPN hydrogels with different fraction of alginate network, it is observed that increased concentration of alginate chains slows down the shrinking process. According to the obtained results, after first 30 min of deswelling process, the percentage of water retained over the dry weight of IPN-1-5-3 equals 465%, while that of IPN-2-5-3 is almost doubled [Fig. 7(b)]. This lower response rate might be caused by more compact and denser structure of IPNs with higher content of CA because of the additional crosslinking of alginate by calcium ions. As a consequence, mobility of PNIPAAm chains in these networks is reduced, and it affects a decrease in the intensity of hydrophobic interactions among isopropyl groups. Hence, the release of entrapped water is the most retarded at hydrogels based on the highest fraction of alginate in comparison with other IPN hydrogels, in spite of strong prevention of skin layer formation. Obtained deswelling curves indicate that the difference in the crosslinking density of PNIPAAm network in IPNs is too low to have a substantial impact on deswelling kinetics of analogous hydrogels.

Reswelling kinetics

Reswelling kinetics of IPN hydrogels was studied in water at 25°C, after they reached equilibrium state at

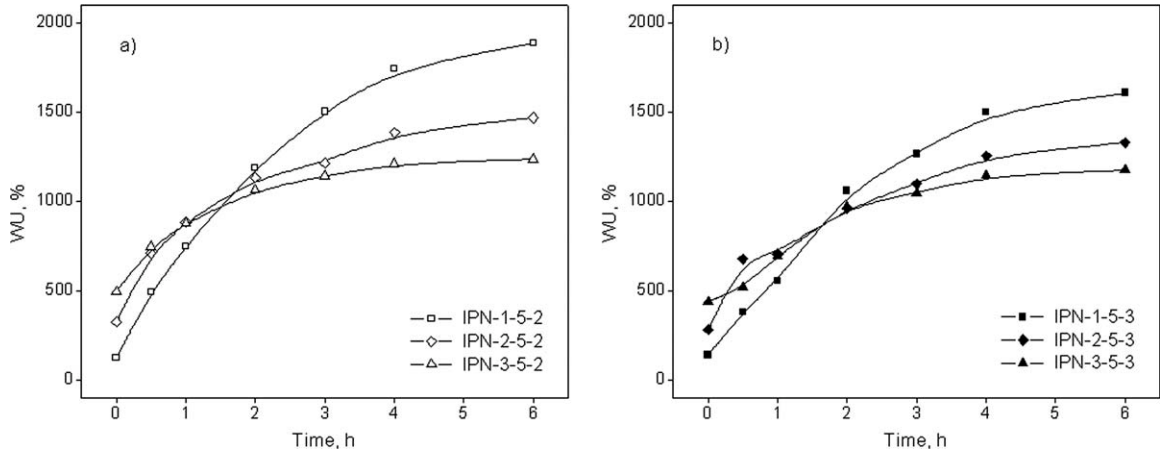

Figure 8 Reswelling kinetics of hydrogels with lower (a) and higher (b) crosslinking degree of PNIPAAm at 25°C.

40°C (Fig. 8). Reswelling profiles of P-0-5-2 and P-0-5-3 hydrogels are not given since it was difficult to manipulate them because of their fragile structure. In the first period of incubation, all analyzed hydrogels have similar trends of reswelling. What is noticeable after 1 h is weaker water uptake ability of hydrogels with higher crosslinking density of PNIPAAm and the same alginate concentration [Fig. 8(b)]. At that time, IPN-1-5-2 has around 26% higher percentage of water uptaken than IPN-1-5-3. Stronger hydrophobic interactions within hydrogel with higher crosslinking degree of PNIPAAm influence the resistance against the influx of water, but only in the first period of reswelling. This is in accordance with the results of other authors who reported that increase in concentration of the crosslinker MBAAm decreases the rate of swelling of the PNIPAAm hydrogels, in case the crosslinker concentration is below 5 wt %.[41]

The IPN hydrogels with lower fraction of alginate feature looser networks enabling increased mobility of polymer chains during rehydration. This leads to a better exposure of hydrophilic segments of polymer chains to water and its easier penetration into the matrix, i.e., rate of water uptake. Hence, after the first hour of reswelling, IPN-1-5-*x* showed around 80% increase in water uptake in comparison with initial equilibrium state at 40°C, whereas this increase was around 60% and 40% for IPN-2-5-*x* and IPN-3-5-*x*, respectively, ($x = 2, 3$). IPN hydrogels based on 1 wt % alginate kept the highest rate of water uptake over other IPN hydrogels until the end of the observed period. After the second hour of reswelling all hydrogels exhibited slowing of water uptake rate, governed by the expansion of polymer chains into the solvent that is more restricted in denser hydrogel matrices.[42] Hydrogels reached equilibrium swollen state after almost 30 h of incubation at 25°C, although the greatest part of swelling capacity is demonstrated after the initial 6 h of reswelling.

Dynamic mechanical properties

The DMA curves in compression mode for different IPN hydrogels are presented in Figures 9–11. The pure PNIPAAm hydrogels have not been analyzed because they were too fragile for adequate manipulation, indicating their mechanically weak structure.

Figure 9 shows the loss and storage moduli as a function of frequency for hydrogel films at 30°C. The storage modulus (G') accounts for an elastic "solid-like" behavior, while the loss modulus (G'') is in relation with viscous properties. In all cases, G' is higher than G'', indicating that elastic properties prevail in all tested hydrogels. Moreover, an improvement in mechanical properties is observed when the alginate content rises, as a result of the increase in overall crosslinking density of hydrogels.

According to Figure 10, an increase in the crosslinking degree of PNIPAAm slightly decreases loss and storage moduli of hydrogels. This confirms that the difference in crosslinking density of PNIPAAm

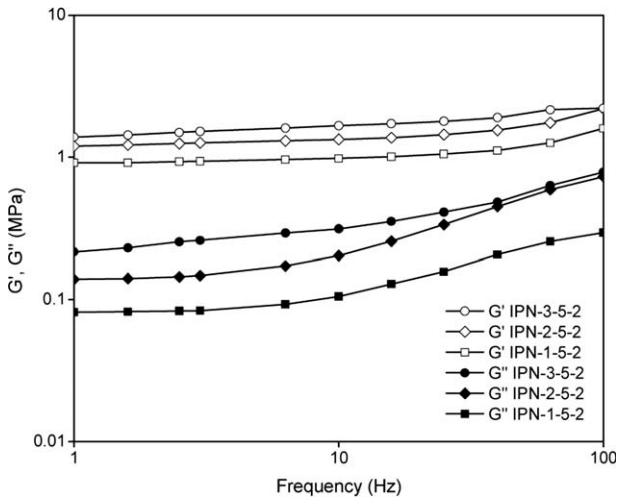

Figure 9 DMA results for IPN hydrogel films below LCST (30°C): influence of alginate content.

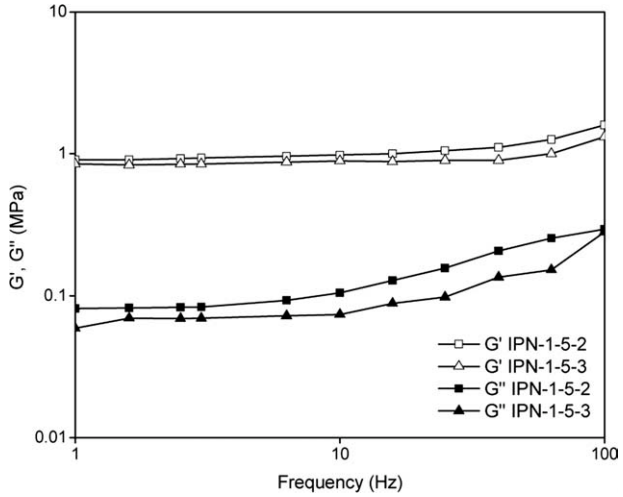

Figure 10 DMA results for IPN hydrogel films below LCST (30°C): influence of crosslinking degree of PNIPAAm.

does not influence the mechanical properties of resulting networks. These results might be also considered as a consequence of the network imperfections. In comparison, the increased concentration of alginate observed above has more emphasized impact on the improvement of dynamic compressive properties (Fig. 9). Analogically, it contributes to a decrease in ESR, as shown earlier (Fig. 5). These phenomena are in agreement with the theory of rubber elasticity which could be applied on hydrogels.[43]

Another set of experiments was done at 40°C. The G' results are compared to those obtained at 30°C for three IPN samples (Fig. 11). At the LCST, analyzed thermosensitive hydrogels undergo volume phase transition and become hydrophobic. According to the results, a large increase in elastic modulus is observed for all hydrogel samples above the LCST, primarily because of the collapse of polymer chains. This phenomenon leads to the formation of a more compact and tight network structure, giving improved mechanical properties. The relative increase in G' is the highest for sample IPN-1-5-3 and the lowest for IPN-3-5-2.

Hydrogel morphology

The pore structure of hydrogels was examined by SEM. Figure 12 shows the SEM micrographs of different hydrogel films with lower crosslinking degree of PNIPAAm, below and above the LCST. The dependence of the interior morphology on hydrogel composition and their thermosensitivity could be clearly seen.

At room temperature, IPN hydrogels with the lowest fraction of alginate feature the most porous structure, even more porous than corresponding pure PNIPAAm hydrogel. High porosity of these IPN samples can be partly explained by the preparation procedure. The initial phase of hydrogel synthesis encompassed 24-h-polymerization and crosslinking of PNIPAAm in the presence of sodium alginate. During this period, electrostatic repulsions among carboxylate anions of alginate chains contribute to the expansion of forming network.[17] This is the case with the samples with the lowest concentration of alginate. In contrast, the structures of IPN samples based on 2 and 3 wt % alginate are more compact than pure PNIPAAm because of the predominant influence of crosslinking of alginate with calcium ions as the last step in their preparation. Hence, these hydrogels feature smaller average pore sizes than pure PNIPAAm hydrogels at 25°C (Fig. 13). This was reflected through the values of ESR at lower temperatures (below the LCST) as well as the results of swelling kinetics (Figs. 5 and 6).

According to given SEM micrographs, IPN matrices become denser and of more emphasized nonuniformity at room temperature with rise in alginate content. It is also clear that the structures of hydrogels become more compact and far less porous after the incubation at 40°C. This can be ascribed to the strong hydrophobic interactions among hydrophobic segments of PNIPAAm, which prevail above the LCST. As a result, the collapse of the polymer chains and restructuring of the hydrogel matrix occurs. Furthermore, it is reported elsewhere that probable formation of the complex between carboxylate groups of CA and amide groups of PNIPAAm is favored at temperatures higher than the LCST.[33] The reason for this can be found in the orientation of apolar isopropyl groups toward the surface of the pores, thus decreasing the interaction with water molecules.

The pore sizes of hydrogels, equilibrium swollen below (25°C) and above (40°C) their LCST are presented in Figure 13. Existence of smaller pores in the

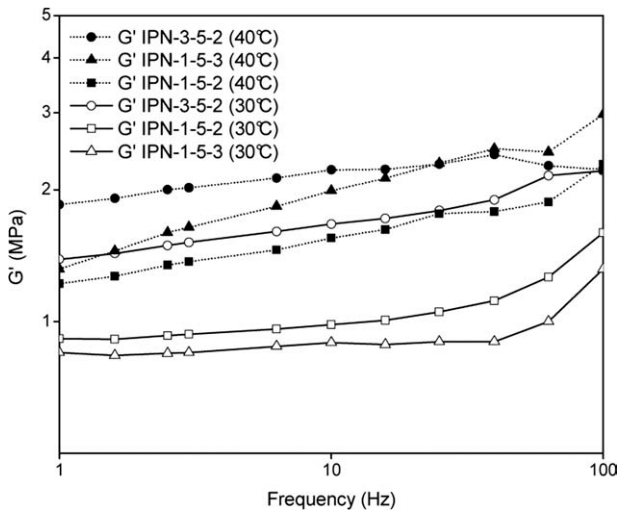

Figure 11 Comparison of DMA results for IPN hydrogel films below and above LCST.

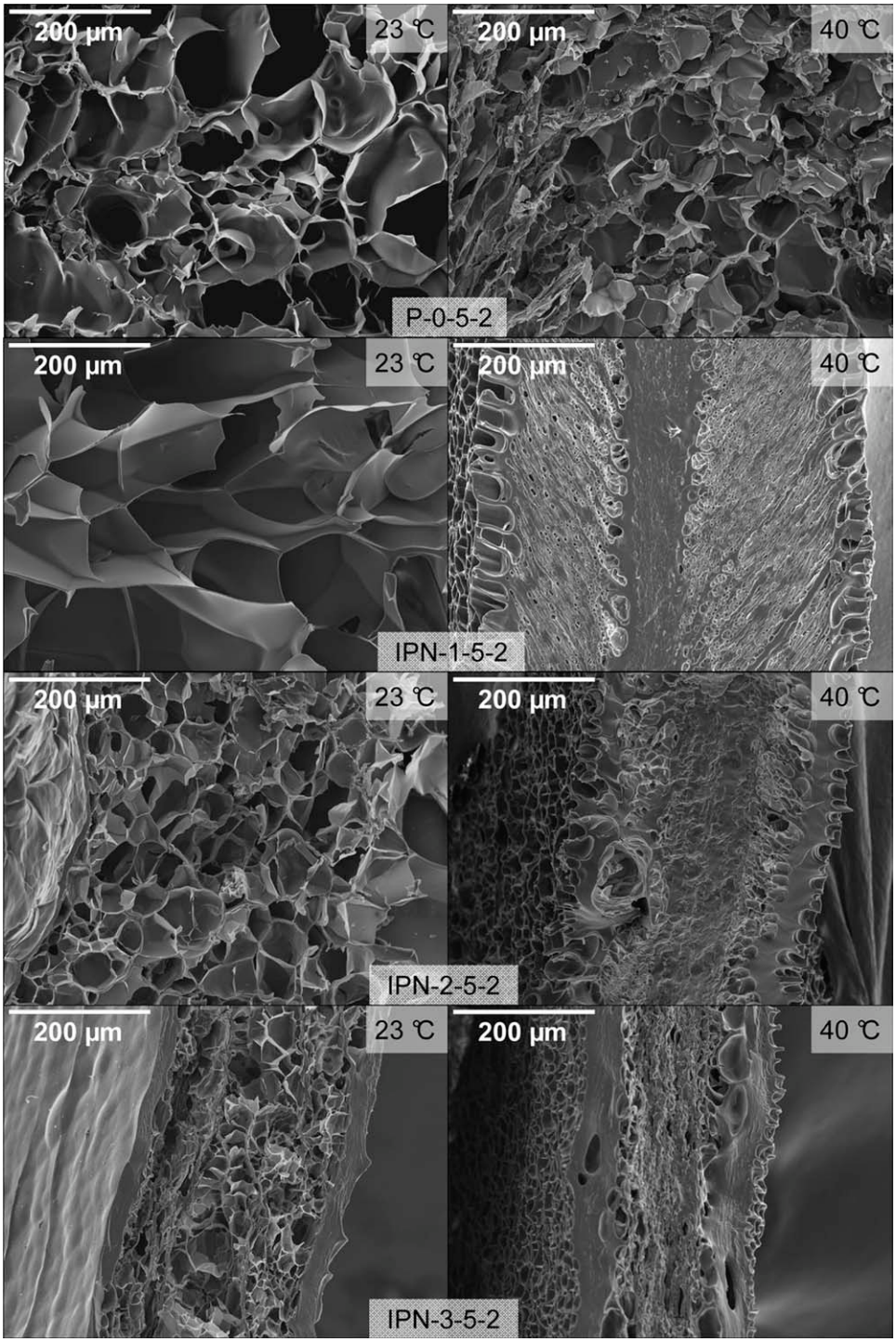

Figure 12 SEM micrographs of hydrogel films: comparison of interior morphology below and above LCST.

structure of IPN hydrogels based on higher alginate content is understandable because of the higher possibility of the intermolecular association for formation of junction points.[44] The most pronounced influence of PNIPAAm crosslinking density is noticed for IPN hydrogels based on 1 and 2 wt % alginate. High standard deviations of pore sizes, as a measure of heterogeneous interior morphology might be the result of steric hindrances[45] caused by higher concentration of alginate chains in the system during free-radical polymerization process of NIPAAm. In addition, inhomogeneous distribution of PNIPAAm crosslinks throughout the hydrogel sample could be induced by this microphase separation. Since MBAAm crosslinker has two vinyl groups, its molecules are incorporated into the growing polymer chains faster then NIPAAm molecules. Hence, network regions formed earlier are more crosslinked are than those formed later.[46]

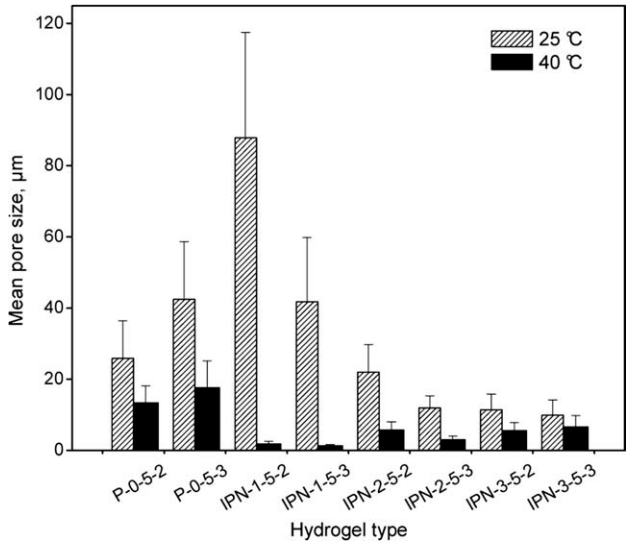

Figure 13 Pore size values of hydrogels at 25°C and 40°C.

The pore size values and SEM micrographs are in accordance with the swelling abilities of hydrogels. The higher is the average pore size of the network the higher is the swelling ratio (Fig. 6). At temperatures above the LCST, pure PNIPAAm hydrogels have the largest pores, which is in accordance with the results of deswelling kinetics. As previously mentioned, the strongest collapse of polymer chains when temperature is raised from 25°C up to 40°C (deswelling) is observed in the case of IPN-1-5-2, corresponding to over 97%-decrease in the average pore size (from around 87 μm down to 2 μm).

Taking into account these results, the IPN hydrogels synthesized in this work could be regarded as supermacroporous or macroporous since they are characterized by pores of micrometer sizes.[47] This macroporosity could be attributed to the impact of the low temperature of NIPAAm polymerization, causing water to remain in the gel phase throughout the polymerization and thus the formation of expanded polymer network.[48]

CONCLUSIONS

The work presented in this article deals with the synthesis and detailed characterization of thermosensitive hydrogels potentially applicable as transdermal drug delivery matrices. Thermal, swelling, mechanical, and morphological properties demonstrated the advantages of IPN hydrogels composed of crosslinked PNIPAAm and CA over pure PNIPAAm hydrogels. The presence of alginate network in IPN hydrogels has no considerable influence on the LCST values (34°C–35°C). CA considerably contributes to the improved strength of the interactions on a molecular level of the IPNs, as indicated by T_g values. The swelling studies showed that increase in alginate content significantly lowers the equilibrium swelling ratios of IPN hydrogels, in particular at temperatures below the LCST. However, IPN hydrogels based on 1 wt % of alginate show better swelling capacity than pure PNIPAAm hydrogels at below the LCST. They also have the most rapid response to temperature increase from 25°C up to 40°C in comparison with other studied hydrogels. The pure PNIPAAm hydrogels exhibit the lowest rate of deswelling because of the formation of dense skin layer. Different crosslinking densities of PNIPAAm have slight impact on the swelling behavior of analogous IPN hydrogels. Higher alginate content contributes to the improved mechanical properties of IPN hydrogels. The same effect is observed when the temperature is increased above the LCST, resulting from the formation of tighter network structures. The IPN hydrogels based on 1 wt % of alginate feature more porous network comparing to pure PNIPAAm hydrogels at 23°C. IPN hydrogels with 1 wt % of alginate also exhibit the greatest changes in pore size values in response to temperature increase. The proper thermosensitivity of IPN hydrogels is a good base for additional study on their combination with heating textiles as a part of drug delivery system for transdermal applications.

References

1. Hoffman, A. S. Adv Drug Delivery Rev 2002, 43, 3.
2. Suzuki, H. J Intell Mater Syst Struct 2006, 17, 1091.
3. Hoare, T. R.; Kohane, D. S. Polymer 2008, 49, 1993.
4. Katayama, S.; Akahori, Y. J Phys Chem 1994, 98, 11115.
5. Chanda, M.; Roy, S. K. Plastics Technology Handbook; CRC Press: Boca Raton, 2007; p 117.
6. Xue, W.; Hamley, I. W. Polymer 2002, 43, 3069.
7. Qiu, Y.; Park, K. Adv Drug Delivery Rev 2001, 53, 321.
8. Koncar, V.; Cochrane, C.; Lewandowski, M.; Boussu, F. Int J Cloth Sci Tech 2009, 21, 82.
9. Nochos, A.; Douroumis, D.; Bouropoulos, N. Carbohydr Polym 2008, 74, 451.
10. Manojlovic, V.; Rajic, N.; Djonlagic, J.; Obradovic, B; Nedovic, V; Bugarski, B. Sensors 2008, 8, 1488.
11. Rinaudo, M. In Polysaccharides: Structural Diversity and Functional Versatility; Dumitriu, S., Ed.; Marcel Dekker: New York, 2005; p 247.
12. Liu, W.; Zhang, B.; Lu, W. W.; Li, X.; Zhu, D.; Yao, K. D.; Wang, Q.; Zhao, C.; Wang, C. Biomaterials 2004, 25, 3005.
13. Muniz, E. C.; Geuskens, G. J Mater Sci Mater Med 2001, 12, 879.
14. Zhang, X. Z.; Wu, D. Q.; Chu, C. C. Biomaterials 2004, 25, 3793.
15. Hernández, R.; Mijangos, C. Macromol Rapid Comm 2009, 30, 176.
16. Ju, H. K.; Kim, S. Y.; Kim, S. J.; Lee, Y. M. J Appl Polym Sci 2002, 83, 1128.
17. Zhang, G.-Q.; Zha, L.-S.; Zhou, M.-H.; Ma, J.-H.; Liang, B.-R. Colloid Polym Sci 2005, 283, 431.
18. Lee, S. B.; Park, E. K.; Lim, Y. M.; Cho, S. K.; Kim, S. Y.; Lee, Y. M.; Nho, Y. C. J Appl Polym Sci 2006, 100, 4439.
19. Guilherme, M. R.; Toledo, E. A.; Rubira, A. F.; Muniz, E.C. J Membr Sci 2002, 210, 129.

20. de Moura, M. R.; Aouada, A. F.; Guilherme, M. R.; Radovanovic, E.; Rubira, A. F.; Muniz, E. C. Polym Test 2006, 25, 961.
21. de Moura, M. R.; Guilherme, M. R.; Campese, G. M.; Radovanovic, E.; Rubira, A. F.; Muniz, E. C. Eur Polym Mater 2005, 41, 2845.
22. de Moura, M. R.; Aouada, F. A.; Favaro, S. L.; Radovanovic, E.; Rubira, A. F.; Muniz, E. C. Mater Sci Eng C 2009, 29, 2319.
23. Shi, J.; Alves, N. M.; Mano, J. F. Macromol Biosci 2006, 6, 358.
24. Feil, H.; Bae, Y. H.; Feijen, J.; Kim, S. W. Macromolecules 1993, 26, 2496.
25. Mohan, Y. M.; Premkimar, T.; Joseph, D. K.; Geckeler, K. E. React Funct Polym 2007, 67, 844.
26. Jeremy, P. K.; Tan, K. C. J Controlled Release 2007, 118, 87.
27. Kim, M. H.; Kim, J. C.; Lee, H. Y.; Kim, J. D.; Yang, J. H. Colloid Surf B 2005, 46, 57.
28. Tam, S. K.; Dusseault, J.; Polizu, S.; Menard, M.; Halle, J. P.; Yahia, L.'H. Biomaterials 2005, 26, 6950.
29. Sakugawa, K.; Ikeda, A.; Takemura, A.; Ono, H. J Appl Polym 2004, 93, 1372.
30. Puttipipatkhachorn, S.; Pongjanyakul, T.; Priprem, A. Int J Pharm 2005, 293, 51.
31. Zhang, X.-Z.; Wu, D.-Q.; Chu, C.-C. J Polym Sci Pol Phys 2003, 41, 582.
32. Grant, G. T.; Morris, E. R.; Rees, D. A.; Smith, P. J. C.; Thom, D. FEBS Lett 1973, 32, 195.
33. de Moura, M. R.; Rubira, A. F.; Muniz, E. C. Polímeros 2008, 18, 132.
34. Erbil, C.; KazancIoglu, E; UyanIk, N. Eur Polym Mater 2004, 40, 1145.
35. Sousa, R. G.; Magalhaes, W. F.; Freitas, R. F. S. Polym Degrad Stabil 1998, 61, 275.
36. Ortega, A.; Bucio, E.; Burillo, G. Polym Bull 2008, 60, 515.
37. Meléndez-Ortiz, H. I.; Bucio, E.; Burillo, G. Radiat Phys Chem 2009, 78, 1.
38. Zhang, X. Z.; Zhuo, R. X. J Colloid Interface Sci 2000, 223, 311.
39. Kaneko, Y.; Yoshida, R.; Sakai, K.; Sakurai, Y.; Okano, T. J Membr Sci 1995, 101, 13.
40. Yoshida, R.; Kaneko, Y.; Sakai, K.; Okano, T.; Sakurai, Y.; Bae, Y. H.; Kim, S. W. J Controlled Release 1994, 32, 97.
41. Sayil, C.; Okay, O. Polymer 2001, 42, 7639.
42. Caykara, T.; Kiper, S.; Demirel, G. Eur Polym Mater 2006, 42, 348.
43. Kloxin, A. M.; Kloxin, C. J.; Bowman, C. N.; Anseth, C. S. Adv Mater 2010, 22, 3484.
44. Hong, P. D.; Chen, J. H. Polymer 1998, 39, 5809.
45. Matyjaszewski, K.; Davis, T. P. Handbook of Radical Polymerization; John Wiley & Sons: Hoboken, 2002.
46. Okay, O. In Smart Polymers: Applications in Biotechnology and Biomedicine; Galaev, I.; Mattiasson, B., Eds.; CRC Press: Roca Baton, 2008; Chapter 9.
47. Mattiasson, B.; Kumar, A.; Galaev, I. Y., Eds.; Macroporous Polymers: Production Properties and Biotechnological/Biomedical Applications; CRC Press: Boca Raton, 2010.
48. Okay, O. In Macroporous Polymers: Production Properties and Biotechnological/Biomedical Applications; Mattiasson, B.; Kumar, A.; Galaev, I. Y., Eds.; CRC Press: Boca Raton, 2010; Chapter 1.